Journal of Neuroscience Methods 214 (2013) 204–209

Contents lists available at SciVerse ScienceDirect

Journal of Neuroscience Methods

journal homepage: www.elsevier.com/locate/jneumeth

Basic Neuroscience

Wireless near-infrared spectroscopy system for determining brain hemoglobin levels in laboratory animals

Jinn-Rung Kuo[a,c,d], Ming-Hsien Chang[b], Che-Chuan Wang[a,b], Chung-Ching Chio[a], Jhi-Joung Wang[d], Bor-Shyh Lin[b,d,*]

[a] Division of Neurosurgery, Department of Surgery, Chi Mei Medical Center, Tainan, Taiwan
[b] Institute of Imaging and Biomedical Photonics, National Chiao-Tung University, Tainan, Taiwan
[c] Department of Biotechnology, Taiwan University of Science and Technology, Tainan, Taiwan
[d] Department of Medical Research, Chi Mei Medical Center, Tainan, Taiwan

HIGHLIGHTS

- The concentration changes of HbO_2, HbR and HbT were significantly related to the traumatic impact strength.
- The infarction volumes after traumatic brain injury were significantly related to the traumatic impact strength.
- A wireless and non-invasive near-infrared spectroscopy system is an alternative tool for determining brain hemoglobin levels in laboratory animals after TBI.

ARTICLE INFO

Article history:
Received 30 November 2012
Received in revised form 27 January 2013
Accepted 28 January 2013

Keywords:
Traumatic brain injury
Near-infrared spectroscopy
Oxyhemoglobin
Deoxyhemoglobin
Total hemoglobin
Triphenyltetrazolium chloride

ABSTRACT

Traumatic brain injury (TBI) is usually caused by brain shaking or impact. It can affect normal brain function and may even lead to disability or death. However, there are very few studies on the associated physiologic changes in humans or animals. In this study, a non-invasive, wireless multi-channel near-infrared spectroscopy (NIRS) was developed to continuously monitor the concentration change of oxyhemoglobin (HbO_2), deoxyhemoglobin (HbR), and total hemoglobin (HbT) to elucidate changes in the physiological state of the brain during and after different strength impaction. The triphenyltetrazolium chloride (TTC) staining was also used to monitor changes of infarction volume after different strength impaction. The results indicated that the concentration changes of HbO_2 and HbT, and the changes of infarction volumes were significantly related to the impact strength. In conclusion, the status of TBI can be clinically evaluated by detecting HbO_2 and HbT changes. The system proposed here is stable, accurate, non-invasive, and mostly important wireless which can easily be used for TBI study.

1. Introduction

Traumatic brain injury (TBI), often due to brain shaking or impact, affects normal brain function and may lead to disability or even death. In the United States, about 1.5 million people suffer from TBI annually (Thurman, 1999), with a financial burden of more than 50 billion U.S. dollars. The associated increase in intracranial pressure (ICP) after TBI leads to a high risk of brain hypoxemia or edema such that a 30% mortality in the first three days has been reported (Noble, 2010). The lack of timely examination and treatment may also lead to death (Ghajar, 2000).

Intracranial pressure monitoring is usually used to monitor TBI. However, its invasive measurement may cause brain hemorrhage and infection (Heegaard and Biros, 2007). Some non-invasive medical instruments, such as magnetic resonance imaging (MRI), computer tomography (CT), and positron emission tomography (PET), may be used to examine TBI (Belanger et al., 2007, Maas et al., 2008), especially to detect cerebral blood flow and acquire information on oxygen metabolism of cerebral tissue. Their limitations include enormous costs and poor mobility, which restrict their practical use in most clinical settings. Moreover, while MRI, which has no ionizing radiation, is safe, it is also the most expensive and its temporal resolution is poorer than that of CT (Hillman, 2007). Both of PET and CT, which require radioactive substance, are unsuitable for long-term monitoring (Crespi, 2007).

Recently, near-infrared spectroscopy (NIRS) was developed and has since been widely applied for cerebral science. The concept of near-infrared spectroscopy was first proposed by Jobsis in 1977

* Corresponding author at: No. 301, Gaofa 3rd Rd., Guiren Dist., Tainan City 711, Taiwan. Tel.: +886 6 3032121x57835; fax: +886 6 3032535.
E-mail addresses: borshyhlin@gmail.com, borshyhlin@mail.nctu.edu.tw (B.-S. Lin).

0165-0270/$ – see front matter © 2013 Elsevier B.V. All rights reserved.
http://dx.doi.org/10.1016/j.jneumeth.2013.01.025

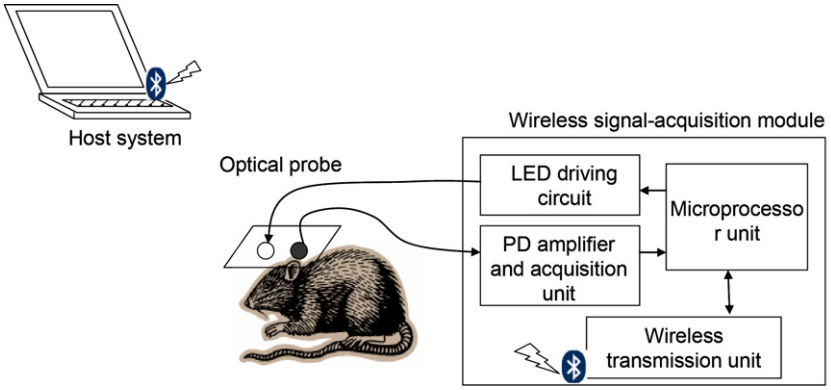

Fig. 1. System architecture of proposed wireless multi-channel NIRS system.

(Jobsis, 1977). For red and near-infrared light, oxyhemoglobin (HbO_2) and deoxyhemoglobin (HbR) are the most significant absorbers in blood or tissue. Using red and near infrared light to penetrate through the brain to monitor their variation of relative optical transparency, the relative concentration changes of HbO_2 and HbR in relation to cerebral blood flow and oxygen metabolism can be calculated. Therefore, near-infrared spectroscopy may be applied to detect focal cerebral ischemia (Tsuji et al., 1998), hemorrhage (Gopinath et al., 1995), stroke (Bönöczk et al., 2002), newborn infant hypoxia (Wyatt et al., 1990), and post-injury cognitive functions (Merzagora et al., 2011). However, up to now, mostly of the devices is wires dependant.

In the present study, a wireless multi-channel NIRS system was designed to monitor changes in HbO_2, HbR, and total-hemoglobin (HbT) concentrations during and after TBI. A TTC staining was also used to monitor changes of infarction volume after different strength impaction. These aimed to clarify the state of brain injury under different impact conditions.

2. Materials and methods

2.1. Design of wireless multi-channel near-infrared spectroscopy system

A wireless multi-channel near-infrared spectroscopy system was designed to monitor changes in the relative HbO_2 and HbR concentrations under TBI. The entire system architecture mainly consisted of a wireless signal acquisition module, an optical probe, and a host system (Fig. 1). The optical probe contained light-emitting diodes (LED) and photodiodes (PD), and was firmly fixed on the subjects. The LED and PD were used to supply the red and infrared light sources, and to transfer the intensity of diffusely reflective light into current or voltage, respectively. The wireless signal acquisition module was designed to drive the red and infrared light sources and to acquire signals obtained from photodiodes. When light was emitted by biological tissue, very little light would penetrate through the tissue due to the scattering and absorbing properties of the different structures. The brain contains five layers (scalp skin, skull, cerebrospinal fluid layer, gray matter, and white matter), and for the wavelength of near-infrared, their scattering coefficients are about 1.9, 1.6, 0.24, 2.2, and 9.1 mm^{-1}, respectively. And the absorption coefficients of the five tissues for near-infrared are about 0.018, 0.016, 0.004, 0.036, and 0.014 mm^{-1}, respectively (Okada and Delpy, 2003). As such, the penetrating light usually carried physiologic information regarding the tissue (Payne et al., 2011). For the wavelength of near-infrared, the absorptions of the five tissues are far less than those of HbO_2 and HbR. Therefore, the absorptions of HbO_2 and HbR are mainly considered in the absorption model.

In general, the penetrating depth of the red and infrared light was about a half of the distance between the light source and the detector (Crespi et al., 2005). The specific area for monitoring HbO_2 and HbR changes could be determined by using this rule. Intensity changes of penetrating red and infrared lights measured by the photodiode was delivered into the wireless signal acquisition module, and then amplified and digitalized. The microprocessor unit in the wireless signal acquisition module calculated the changes of HbO_2 and HbR by using a modified Beer-Lambert law (MBLL). The differential path-length factor (DPF) used in MBLL is a scaling factor relating to the light source-detector distance to the true optical path-length traveled by the scattered light (Boas et al., 2001, van der Zee et al., 1992), and can be expressed by,

$$B = \frac{1}{2}\left(\frac{3\mu_s'}{\mu_a^{initial}}\right)^{1/2}\left[1 - \frac{1}{(1 + L(3\mu_s'^{initial}\mu_a^{inital})^{1/2}}\right] \quad (1)$$

where μ_s' is the transport scattering coefficient, μ_a is the absorption coefficient, and L denotes the light source-detector distance. And the relative change Δ[HbT] of total-hemoglobin from its baseline can then be calculated by using the formula:

$$\Delta[\mathrm{HbT}] = \Delta[\mathrm{HbO_2}] + \Delta[\mathrm{HbR}] \quad (2)$$

where $\Delta[HbO_2]$ and Δ[HbR] represented the relative concentration changes of HbO_2 and HbR from their baseline, respectively. These data were then transmitted into a computer or wireless handheld device.

2.1.1. Optical probe

Most near-infrared spectroscopy systems used laser diodes and avalanche photodiodes combined with a fiber-optic module as the optical probe (Culver et al., 2003). Instead of laser diodes and avalanche photodiodes, surface mounted device (SMD) LED (SMT735/850, EPITEX, Japan) and silicon-pin PD (PD15-22 C/TR8, EVERLIGHT, Taiwan), which were low-cost, safe and small-volume, were used as the light source and the detector, respectively. These were embedded in the optical probe to effectively maintain contact with the head of subject (Fig. 2). Through the module design of the probe, the number of LEDs and PDs were easily selected for different applications.

2.1.2. Wireless signal acquisition module

The wireless signal acquisition module mainly consisted of a microprocessor unit, a LED driving circuit, a PD amplifier and acquisition unit, and a wireless transmission unit. Texas Instruments MSP430, with the advantage of ultra-low power consumption and high operation performance, was used as the microprocessor unit. The wireless transmission unit consisted of a Bluetooth module, with Bluetooth v2.0 compliant specification, and an antenna on

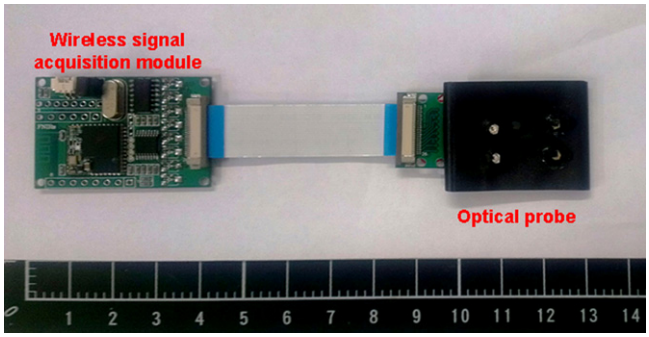

Fig. 2. Photographs of proposed optical probe and wireless signal acquisition module.

the Printed Circuit Board (PCB). The LED driving circuit consisted of a multiplexer, operation amplifiers, and NPN transistors. The multiplexer was used as a LED selector that received the control command from the microprocessor unit to turn on or turn off the LED. The operation amplifier was used to stabilize the voltage on the emitter of the NPN transistor to provide a steady current passing through these LED.

In the PD amplifier and acquisition unit, a 20 M trans-resistance amplifier was designed to convert the PD current into voltage signal, and a low-pass filter with the cut-off frequency of 1.5 kHz was designed to reduce high frequency noise. The amplified PD signal was digitized by an analog-to-digital converter (ADC) built in the microprocessor unit. The sampling rate of ADC was set to 25 Hz in this module. After digitizing the PD signal, the microprocessor unit then calculated the $\Delta[HbO_2]$ and $\Delta[HbR]$ by using the modified Beer-Lambert law and transmit the results of $\Delta[HbO_2]$ and $\Delta[HbR]$ to the host system wirelessly via Bluetooth. The firmware program (Fig. 3) was embedded in the wireless signal acquisition module,

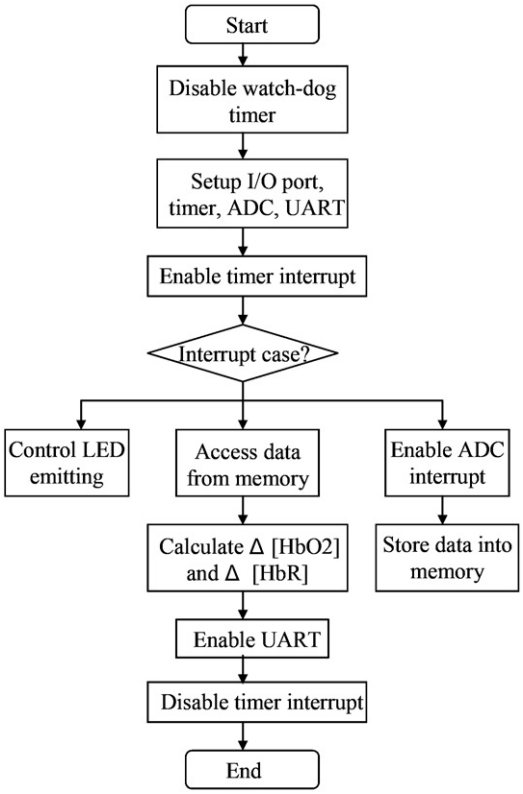

Fig. 3. Operation procedure of the firmware program in the wireless signal acquisition module.

which operated at 100 mA with 3.7 V DC supply using a 3.7-V 1100-mAh lithium battery that could last for over 10 h. The wireless signal acquisition module was about 40 mm × 29 mm × 5 mm in size.

2.1.3. Host system

A commercial laptop was used as the platform of the host system, with Windows 7 as the operating system. The real-time monitoring program developed by Microsoft Visual C# was designed to receive real-time HbO_2 and HbR concentrations. The software architecture of the real-time monitoring program had three main parts: GUI, BUFFER and THREAD. GUI was the base of any graphical user interface (GUI) and the form and panel extending from the GUI provided the ability to precisely control the location and display of the GUI elements. BUFFER was a container used to store data received from the wireless signal acquisition module and other system setting parameters. THREAD had two independent threads: Bluetooth API and NIRS REC. Bluetooth API established the Bluetooth communication between the wireless signal acquisition module and the system platform, while NIRS REC received raw data from the wireless signal acquisition module and stored them into BUFFER.

Initially, the program built a GUI that allowed the user to set program parameters and select the monitoring channel. The program then called the Bluetooth DeviceInfo function in the Bluetooth API to search the wireless signal acquisition module. When the wireless signal acquisition module was found, the serial port profile (SPP) protocol service was registered, and the system platform connected to the wireless signal acquisition module to receive data on the diffusely reflected light and store them into BUFFER.

2.2. Animals preparation

Adult male Sprague Dawley rats (weight, 375 ± 25 g) were prepared for the experiments. All of the rats were kept under a 12-hour light/dark cycle and allowed to access to food and water freely. All experimental procedures conformed to the guidelines of the National Institute of Health, Taiwan and were approved by the Animal Care and Use Committee of Chi-Mei Medical Center to minimize discomfort to animals during surgery and recovery periods.

The rats were randomly assigned to three groups under the fluid percussion injury experiment with different impacts (1.6 atm, 2.0 atm, and 2.4 atm) using the NIRS system. All of the rats were anesthetized with sodium pentothal (25 mg/kg, i.p.; Sigma Chemical Co, St. Louis, MO) and a mixture containing ketamine (44 mg/kg, i.m.; Nan Kuang Pharmaceutical, Tainan, Taiwan), atropine (0.02633 mg/kg, i.m.; Sintong Chemical Industrial Co, Ltd, Taoyuan, Taiwan), and xylazine (6.77 mg/kg, i.m.; Bayer, Leverkusen, Germany). All of the rats were sacrificed on the third day post-surgery and rat brain slices were stained by triphenyltetrazolium chloride (TTC) solution.

2.3. Experimental design for traumatic brain injury

The fluid percussion injury (FPI) experiment was used as the rat model for TBI (Thompson et al., 2005). Before beginning the FPI experiment, the rat was anesthetized and its head was placed in a stereotaxic frame while its ears were held by ear bars to tighten its head. A rectal temperature probe was inserted into the colon of the rat and attached to the thermostatic controller that powered the heating pad to maintain the rat core temperature at 37 °C. The fur on the rat head was trimmed, and the scalp was incised sagittally. In order to focus on the rat brain directly, a hole on the skull was drilled anterior-posterior −3 mm and lateral +4 mm from the bregma to expose the rat brain. A leur-lock connector was cemented to the craniotomy with cyanoacrylic adhesive and dental acrylic, while the other side of the connector was connected with a sealed and

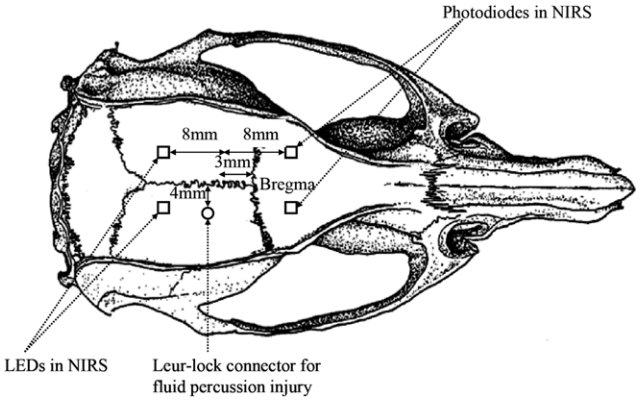

Fig. 4. Monitoring positions for NIRS were at striatum region of rat brain, anterior-posterior −0.5 mm and lateral +3.5 mm from bregma, under top of rat brain 8 mm (includes 1 mm rat skull). Distance between LEDs and PDs was set to 16 mm.

fluid-filled reservoir. Then a pendulum struck the reservoir to generate a fluid wave to hit the rat brain and form fluid percussion injury. (Fig. 4) illustrates the location of placing the NIRS probe and the leur-lock connector.

Before beginning the FPI experiment, the changes of 30-s HbO_2 and HbR were recorded as baseline data. The FPI experiment was then applied to the rat. After the FPI experiment, the rat was removed from the FPI device. Since tranisent apnea occurred after FPI, a respiratory treatment procedure by withdrawing the rat's tongue out of mouth was performed immediately after FPI for protect the airway patent (Kuo et al., 2007). The respiratory treatment period is defined as from withdrawing the tongue out of the mouth to start spontaneous respiration. The HbO_2 and HbR changes of the brain-injured rat were monitored continuously for 2 h. After all experimental procedures, the connector and the acrylic on the rat head were removed and the incisions on the rat were sutured.

2.4. Cerebral infarction assay

The triphenyltetrazolium chloride (TTC) staining procedures were as described previously (Kuo et al., 2011). All animals after different strength impacts were sacrificed 72 h after TBI. The volume of infarction, as revealed by negative TTC stains indicating dehydrogenase-deficient tissue, was measured in each slice and summed using computerized planimetry (PC-based Image Tools software). The volume of infarction was calculated as 2 mm (thickness of the slice) × [sum of the infarction area in all brain slices (mm^2)].

2.5. Statistical analysis

Physiologic data were analyzed with repeated-measure ANOVA for differences between time points and groups. Significance was set at $p < 0.05$. Data were expressed as mean ± standard error of the mean.

3. Results

The real-time changes of $\Delta[HbO_2]$, Δ[HbR], and Δ[HbT] in ipsilateral side during and after FPI experiment were obtained (Fig. 5). In our previous experiment, the 5-min raw data before traumatic brain injury experiment have been monitored. We found that the 5-min relative changes of HbO_2 and HbR before experiment for the anesthetized rats are very stable. Therefore, the 30-s raw data before experiment were used as the baseline in this study. Moreover, from the experimental results, it also clearly shows that the effect of respiratory treatment on the short-term changes of

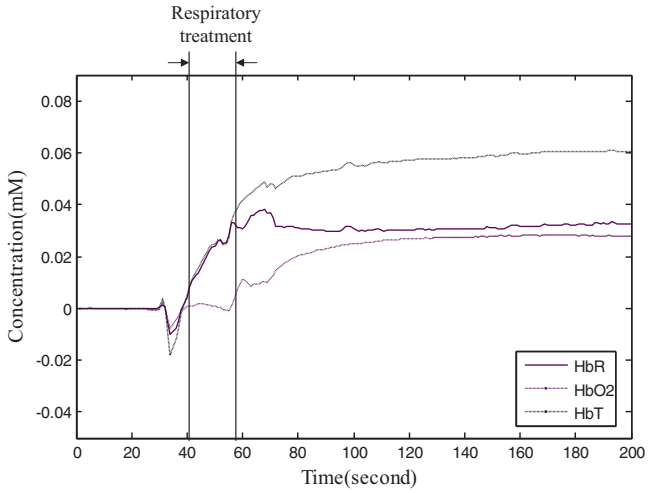

Fig. 5. Real-time change of $\Delta[HbO_2]$, Δ[HbR], and Δ[HbT] in ipsilateral side during and after FPI experiment.

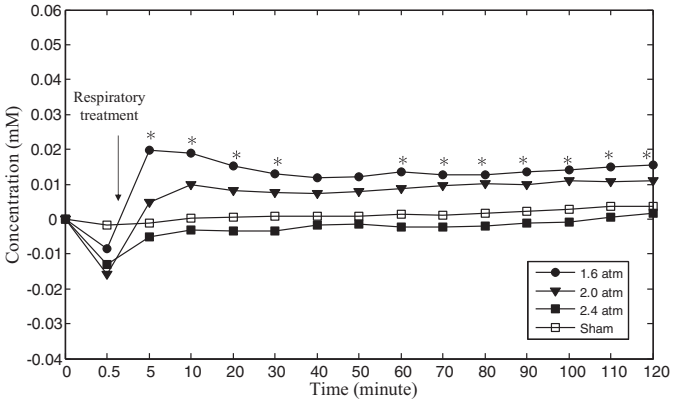

Fig. 6. Time courses of Δ[HbO] corresponding to different impact strengths (* means significance).

$\Delta[HbO_2]$, Δ[HbR], and Δ[HbT] is small during the period of respiratory treatment.

The temporal profiles of $\Delta[HbO_2]$, Δ[HbR], and Δ[HbT] were obtained from the ipsilateral and contralateral sides (Figs. 6–8) during and after the FPI experiment. Here, the raw data of $\Delta[HbO_2]$, Δ[HbR], and Δ[HbT] were preprocessed by a low-pass filter (moving average filter with 1-s window) to monitor their changing trend. The raw data were statistically analyzed every 10 min. In order to

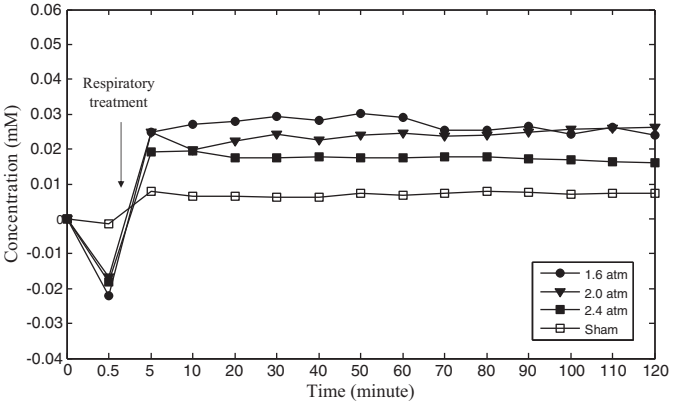

Fig. 7. Time courses of Δ[HbR] corresponding to different impact strengths (* means significance).

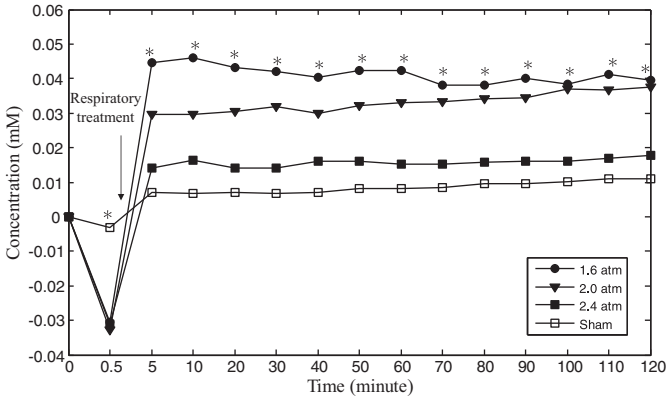

Fig. 8. Time courses of Δ[HbT] corresponding to different impact strengths (* means significance).

monitor the short-term change of the raw data, the time point of impact (at about 0.5 min) and 4.5 min after impact (at about 5 min) were also statistically analyzed. Both $\Delta[HbO_2]$ and Δ[HbR] dropped immediately upon impact and both of $\Delta[HbO_2]$ and Δ[HbR] tended to increase during the period of respiration treatment and even increased compared to their baseline levels after the respiration treatment. During and after the respiration treatment, Δ[HbT] also increased. Variations of $\Delta[HbO_2]$ and Δ[HbR] in the contralateral side were also slightly affected by the impact.

The effect of the impact strength on the change of the infarction volume was investigated. Here, ANOVA was used to analyze the infarction volume corresponding to different impact strengths. The statistic results of the infarction volume corresponding to different impact strengths indicated that the higher impact strength caused a larger region of infarction volume (Fig. 9). The averages and standard deviations of the infarction volumes for 1.6 atm, 2.0 atm and 2.4 atm are $67.75 \pm 14.88\,mm^3$, $86.6 \pm 24.84\,mm^3$, $138 \pm 7.07\,mm^3$ respectively. And the differences between the infarction volumes for 2.4 atm and other impact strengths (1.6 atm and 2.0 atm) are significant. This proved that the severity of TBI (infarction volume) in this experiment can exactly be controlled by adjusting the impact strength.

Repeated-measure ANOVA for differences between time points and groups was used to analyze experimental data. The impact strengths were set from 1.6 atm to 2.4 atm. The changes of $\Delta[HbO_2]$ and Δ[HbT] corresponding to different impact strengths were significant but the relationships between the impact strengths and the concentration changes of $\Delta[HbO_2]$, Δ[HbR], and Δ[HbT] in the ipsilateral side at the moment of impact were not linear and significantly different from those of the contra lateral side. Subsequently, common tendencies of concentration changes in $\Delta[HbO_2]$, Δ[HbR], and Δ[HbT] for different impact strengths were increasing and became gradually stable.

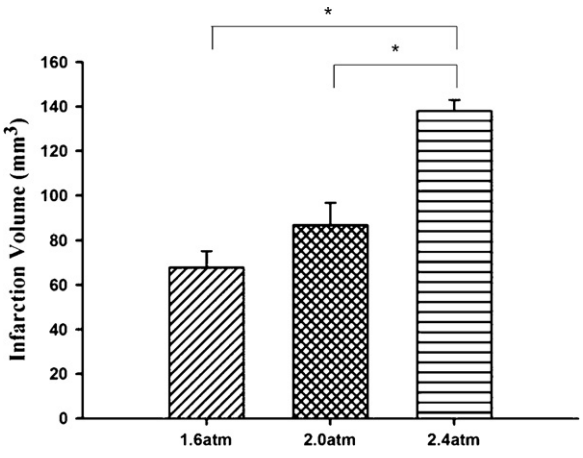

Fig. 9. Infarction volume statistics after brain slices stained by TTC solution in different impact strengths (symbol * means significance).

4. Discussions

Traumatic head injury may cause the direct mechanical damage such as vessels distortion and cells damage initially, followed by influence the cerebral blood flow (hypo- and hyperperfusion), inadequate cerebral oxygenation, impairment of cerebrovascular auto-regulation (vessels constriction or dilate to maintain adequate blood flow for metabolic demand), cerebral metabolic dysfunction, and finally may lead to apoptotic and necrotic cell death. (Werner and Engelhard, 2007, Pierro et al., 2012).

As Figs. 6–8 demonstrated that common tendencies of $\Delta[HbO_2]$, Δ[HbR], and Δ[HbT] for different impact strengths in the ipsilateral side abrupt drop initially, and then increase and become stable gradually when using percussion injury forces 1.6 atm. These initially abrupt dropped of $\Delta[HbO_2]$, Δ[HbR], and Δ[HbT] after FPI could be resulted from post-FPI apnea causing no oxygen from lung to systemic circulation, the impact pressure may result in distortion or displacement of the cerebral vasculature, and finally lead to an immediate decrease in cerebral blood flow corresponding to cerebral hypoperfusion (McIntosh et al., 1996; Martin et al., 1997). That cerebral hypoperfusion immediately after FPI is consistent with the idea that decrease cerebral blood flow or volume is related to decrease Δ[HbT] (Wyatt et al., 1986) as our data presented.

However, the $\Delta[HbO_2]$, Δ[HbR], and Δ[HbT] on the ipsilateral side tended to increase during (averagely about 38.8 ± 9.0 s) and after the period of respiration treatment. Overall, these phenomena maybe resulted from post-hypoperfusion followed by hyperperfusion for metabolic demand (Andersen and Marmarou, 1992; Hovda et al., 1995, Pierro et al., 2012) by an effective auto-regulation. The increase in Δ[HbT] can be explained by vascular dilation and the perfusion phenomenon in the presence of effective auto-regulation. The Δ[HbR] is obviously larger than the $\Delta[HbO_2]$, which may be owing to the brain cells within the optic field were in ischemia conditions requiring more oxygen to promote cell survival, which is consistent previous report (Liu et al., 2008; Marchal et al., 1999). On the contralateral side, variations in $\Delta[HbO_2]$ and Δ[HbR] are also slightly affected by the impact. The results reveal that impact pressure can be transmitted to the contralateral side and may also cause slight brain injury and then alter neurotransmitter activities on the contralateral side (Crespi and Pietra, 1997).

In order to evaluate the effects of impact strength on $\Delta[HbO_2]$, Δ[HbR], Δ[HbT], and infarction volume, we further designed another 2.0 and 2.4 atm fluid percussion injury. As Figs. 6–8 demonstrated, the impact strength of 2.4 atm is set as the highest strength in the FPI experiment and is usually regarded as severe TBI (Vitarbo et al., 2004). After receiving a 2.4 atm impact, Δ[HbR] and Δ[HbT] concentrations increased to levels much higher than their baseline, but the concentration of $\Delta[HbO_2]$ became lower than baseline. These data supported the concept that ischemia-like pattern after FPI could occur as middle cerebral artery occlusion did in animal model (Liu et al., 2008). When compared Δ[HbT] in 2.4 atm with 1.6 and 2.0 atm imapct, it showed the increase in Δ[HbT] after the 2.4 atm impact was significantly smaller than those of 1.6 and 2.0 impact strengths. Furthermore, the $\Delta[HbO_2]$ after the 2.4 atm impact was significantly lower than those of 1.6 and 2.0 impact strengths. We supposed vascular dilation is not enough to provide sufficient blood flow into the injured region after 2.4 amt impact. Thus, the increase in $\Delta[HbO_2]$ cannot provide sufficient oxygen to satisfy the requirements of metabolism. These

results were supported by TTC staining which revealed that impact with 2.4 atm had the largest damage and infarction volume (Fig. 9).

5. Conclusions

Regarding traumatic brain injury (TBI), concentration changes in $\Delta[HbO_2]$,Δ[HbR], and Δ[HbT] decrease immediately at the moment of impact and increased gradually after respiration treatment. Moreover, the experimental results also indicate that the concentrations of $\Delta[HbO_2]$, Δ[HbR], and Δ[HbT] after impact significantly depend on impact strength. Concentrations of $\Delta[HbO_2]$, Δ[HbR], and Δ[HbT] after impact tend to decrease with increasing impact strength. Therefore, a wireless and non-invasively monitoring the concentration changes of $\Delta[HbO_2]$, Δ[HbR], and Δ[HbT] using NIRS may be useful for evaluating the state of TBI in the clinical setting.

Acknowledgement

The authors would like to acknowledge the financial support of the National Science Council of the Republic of China (Grant No. NSC 101-2221-E-009-039).

References

Andersen BJ, Marmarou A. Post-traumatic selective stimulation of glycolysis. Brain Res 1992;585:184–9.
Bönöczk P, Panczel G, Nagy Z. Vinpocetine increases cerebral blood flow and oxygenation in stroke patients: a near-infrared spectroscopy and trans-cranial Doppler study. Eur J Ultrasound 2002;15:85–91.
Belanger H, Vanderploeg R, Curtiss G, Warden D. Recent neuro-imaging techniques in mild traumatic brain injury. J Neuropsychiatry Clin Neurosci 2007;19:5–20.
Boas DA, Gaudette T, Strangman G, Cheng X, Marota JJ, Mandeville JB. The accuracy of near infrared spectroscopy and imaging during focal changes in cerebral hemodynamics. Neuroimage 2001;13(1):76–90.
Crespi F, Pietra C. Middle cerebral artery occlusion alters neurotransmitter activities in ipsilateral and contralateral rat brain regions: an ex vivo voltammetric study. Neurosci Lett 1997;230(2):77–80.
Crespi F, Bandera A, Donini M, Heidbreder C, Rovati L. Non-invasive in vivo infrared laser spectroscopy to analyse endogenous oxy-haemoglobin, deoxy-haemoglobin, and blood volume in the rat CNS. J Neurosci Methods 2005;145:11–22.
Crespi F. Near-infrared spectroscopy (NIRS): a non-invasive in vivo methodology for analysis of brain vascular and metabolic activities in real time in rodents. Curr Vasc Pharmacol 2007;5:305–21.
Culver JP, Durduran T, Furuya D, Cheung C, Greenberg JH, Yodh A. Diffuse optical tomography of cerebral blood flow, oxygenation, and metabolism in rat during focal ischemia. J Cereb Blood Flow Metab 2003;23:911–24.
Ghajar J. Traumatic brain injury. Lancet 2000;356:923–9.
Gopinath SP, Robertson CS, Contant CF, Narayan RK, Grossman RG, Chance B. Early detection of delayed traumatic intra-cranial hematomas using near-infrared spectroscopy. J Neurosurg 1995;83:438–44.
Heegaard W, Biros M. Traumatic brain injury. Emerg Med Clin North Am 2007;25:655–78.
Hillman EMC. Optical brain imaging in vivo: techniques and applications from animal to man. J Biomed Opt 2007;12:051402.
Hovda DA, Lee SM, Smith ML, et al. The neurochemical and metabolic cascade following brain injury: moving from animal models to man. J Neurotrauma 1995;12:903–6.
Jobsis FF. Non-invasive, infrared monitoring of cerebral and myocardial oxygen sufficiency and circulatory parameters. Science 1977;198:1264–7.
Kuo JR, Lo CJ, Chio CC, Chang CP, Lin MT. Resuscitation from experimental traumatic brain injury by agmatine therapy. Resuscitation 2007;75:506–14.
Kuo JR, Lo CJ, Chang CP, Lin KC, Lin MT, Chio CC. Agmatine-promoted angiogenesis, neurogenesis, and inhibition of gliosis-reduced traumatic brain injury in rats. J Trauma 2011;71:E87.
Liu LF, Yeh CK, Chen CH, Wong TW, Jason Chen JJ. Measurement of cerebral blood flow and oxygen saturation using laser Doppler flowmetry and near infrared spectroscopy in ischemia stroke. J Med Biol Eng 2008;28(2):101–5.
Maas AIR, Stocchetti N, Bullock R. Moderate and severe traumatic brain injury in adults. Lancet Neurol 2008;7:728–41.
Marchal G, Young AR, Baron JC. Early postischemic hyperperfusion: pathophysiologic insights from positron emission tomography. J Cereb Blood Flow Metab 1999;19(5):467–82.
Martin NA, Patwardhan RV, Alexander MJ, et al. Characterization of cerebral hemodynamic phases following severe head trauma: hypoperfusion, hyperemia, and vasospasm. J Neurosurg 1997;87:9–19.
McIntosh TK, Smith DH, Meaney DF, Kotapka MJ, Gennarelli TA, Graham DI. Neuropathological sequelae of traumatic brain injury: relationship to neurochemical and biochemical mechanisms. Lab Invest 1996;74:315–42.
Merzagora AC, Schultheis MT, Onaral B, Izzetoglu M. Functional near-infrared spectroscopy based assessment of attention impairments after traumatic brain injury. J Innov Opt Health Sci 2011;4:251–60.
Noble KA. Traumatic Brain Injury and Increased Intracranial Pressure. J Perianesth Nurs 2010;25:242–50.
Okada E, Delpy DT. Near-infrared light propagation in an adult head model. I. Modeling of low-level scattering in the cerebrospinal fluid layer. Appl Opt 2003;42:2906–14.
Payne SJ, Mohammad J, Tisdall MM, Tachtsidis I. Effects of arterial blood gas levels on cerebral blood flow and oxygen transport. Biomed Opt Express 2011;2(4):966–79.
Pierro ML, Sassaroli A, Bergethon PR, Ehrenberg BL, Fantini S. Phase-amplitude investigation of spontaneous low-frequency oscillations of cerebral hemodynamics with near-infrared spectroscopy: a sleep study in human subjects. Neuroimage 2012;63(3):1571–84.
Thompson HJ, Lifshitz J, Marklund N, Grady MS, Graham DI, Hovda DA, et al. Lateral fluid percussion brain injury: a 15-year review and evaluation. J Neurotrauma 2005;22:42–75.
Thurman D.J., Traumatic brain injury in the United States: a report to congress. Centers for Disease Control and Prevention; 1999.
Tsuji M, Duplessis A, Taylor G, Crocker R, Volpe JJ. Near-infrared spectroscopy detects cerebral ischemia during hypotension in piglets. Pediatr Res 1998;44:591–5.
van der Zee P, Cope M, Arridge SR, Essenpreis M, Potter LA, Edwards AD, et al. Experimentally measured optical pathlengths for the adult head, calf and forearm and the head of the newborn infant as a function of inter optode spacing. Adv Exp Med Biol 1992;316:143–53.
Vitarbo EA, Chatzipanteli K, Kinoshita K, Truettner JS, Alonso OF, Dietrich WD. Tumor necrosis factor [alpha] expression and protein levels after fluid percussion injury in rats: the effect of injury severity and brain temperature. Neurosurgery 2004;55:416–25.
Werner C, Engelhard K. Pathophysiology of traumatic brain injury. Br J Anaesth 2007;99:4–9.
Wyatt J, Cope M, Delpy D, Richardson C, Edwards A, Wray S, et al. Quantitation of cerebral blood volume in human infants by near-infrared spectroscopy. J Appl Physiol 1990;68:1086–91.
Wyatt J, Delpy D, Cope M, Wray S, Reynolds E. Quantification of cerebral oxygenation and haemodynamics in sick newborn infants by near-infrared spectrophotometry. Lancet 1986;328:1063–6.